Shape Sensitivity Analysis of Linear-Elastic Cracked Structures Under Mode-I Loading

Guofeng Chen

Sharif Rahman
e-mail: rahman@engineering.uiowa.edu

Department of Mechanical Engineering,
The University of Iowa,
Iowa City, IA 52242
website:
http://www.engineering.uiowa.edu/~rahman

Young Ho Park
Department of Mechanical Engineering,
New Mexico State University,
Las Cruces, NM 88003

A new method is presented for shape sensitivity analysis of a crack in a homogeneous, isotropic, and linear-elastic body subject to mode-I loading conditions. The method involves the material derivative concept of continuum mechanics, domain integral representation of the J-integral, and direct differentiation. Unlike virtual crack extension techniques, no mesh perturbation is needed in the proposed method. Since the governing variational equation is differentiated prior to the process of discretization, the resulting sensitivity equations are independent of any approximate numerical techniques, such as the finite element method, boundary element method, or others. Since the J-integral is represented by domain integration, only the first-order sensitivity of displacement field is needed. Two numerical examples are presented to illustrate the proposed method. The results show that the maximum difference in calculating the sensitivity of J-integral by the proposed method and reference solutions by analytical or finite-difference methods is less than three percent. [DOI: 10.1115/1.1486017]

Introduction

For structures containing cracks, the stress-intensity factor (SIF) and energy release rate (ERR) are the well-known fracture parameters in linear-elastic fracture mechanics (LEFM). If an asymptotic crack-tip solution with a free amplitude parameter exists, the strength of the stress and strain fields near the crack tip can be expressed in terms of these parameters. Hence, these fracture parameters provide a mechanistic relationship between the residual strength of a structural component to the size and location of a crack—either real or postulated—in that component. However, in some applications of fracture mechanics, derivatives of SIF or ERR with respect to crack size are needed for predicting stability and arrest of crack propagation. Another major use of the derivatives of SIF or ERR is in the reliability analysis of cracked structures. For example, the first and second-order reliability methods [1], frequently used in PFM [2–4], require the gradient and Hessian of the performance function with respect to the crack length. In LEFM, the performance function builds on SIF or ERR. Hence, both first and second-order derivatives of SIF or ERR are needed for probabilistic analysis. Therefore, an important requirement of PFM is to evaluate the rates of SIF and ERR accurately and efficiently.

Some methods have already appeared for predicting sensitivities of SIF or ERR. In 1988, Lin and Abel [5] introduced a direct-integration approach of the virtual crack extension technique [6–8] that employs variational formulation and the finite element method (FEM) to calculate the first-order derivative of SIF for a structure containing a single crack. Subsequently, Hwang et al. [9] generalized this method to calculate both first and second-order derivatives for structures involving multiple crack systems, axisymmetric stress state, and crack-face and thermal loading. A salient feature of this method is that SIFs and their derivatives can be evaluated in a single analysis. However, this method requires mesh perturbation—a fundamental requirement of all virtual crack extension techniques. For second-order derivatives, the number of elements surrounding the crack tip that are affected by mesh perturbation has a significant effect on the solution accuracy [9]. Recently, Feijóo et al. [10] applied concepts of shape sensitivity analysis [11] to calculate the first-order derivative of the potential energy. Since ERR is the first derivative of potential energy, this approach can be used to calculate the ERR without any mesh perturbation. Taroco [12] later extended this approach to formulate the second-order sensitivity of the potential energy in predicting the first-order derivative of the ERR; however, this is a difficult task, since the calculation of second-order sensitivities of stress and strain is involved. It is worth mentioning that no numerical results of the sensitivity of ERR were reported by Taroco [12].

This paper presents a new method for predicting the first-order sensitivity of the *J*-integral for a crack in a homogeneous, isotropic, and linear-elastic structure subject to mode-I loading conditions. The method involves the material derivative concept of continuum mechanics, domain integral representation of the *J*-integral, and direct differentiation. Two numerical examples are presented to calculate the first-order derivative of the *J*-integral, using the proposed method. The results from this method are compared with results from the analytical or the finite-difference method.

Shape Sensitivity Analysis

Velocity Field. Consider a general three-dimensional body with a specific configuration, referred to as the reference configuration, with domain Ω, boundary Γ, and a body material point identified by position vector $\mathbf{x}\in\Omega$. Consider the motion of the body from the configuration with domain Ω and boundary Γ into another configuration with domain Ω_τ and boundary Γ_τ, as shown in Fig. 1. This process can be expressed as

$$\mathbf{T}:\mathbf{x}\rightarrow\mathbf{x}_\tau, \quad \mathbf{x}\in\Omega \tag{1}$$

where $\mathbf{x}$ and $\mathbf{x}_\tau$ are the position vectors of a material point in the reference and perturbed configurations, respectively, $\mathbf{T}$ is a transformation mapping, and τ is a timelike parameter with

$$\mathbf{x}_\tau=\mathbf{T}(\mathbf{x},\tau), \quad \Omega_\tau=\mathbf{T}(\Omega,\tau), \quad \Gamma_\tau=\mathbf{T}(\Gamma,\tau) \tag{2}$$

A velocity field $\mathbf{V}$ can then be defined as

$$\mathbf{V}(\mathbf{x}_\tau,\tau)=\frac{d\mathbf{x}_\tau}{d\tau}=\frac{d\mathbf{T}(\mathbf{x},\tau)}{d\tau}=\frac{\partial\mathbf{T}(\mathbf{x},\tau)}{\partial\tau} \tag{3}$$

Contributed by the Pressure Vessels and Piping Division and presented at the Pressure Vessels and Piping Conference, Seattle, Washington, July 23–27, 2000, of THE AMERICAN SOCIETY OF MECHANICAL ENGINEERS. Manuscript received by the PVP Division, May 14, 2001; revised manuscript received April 15, 2002. Associate Editor: K. K. Yoon.

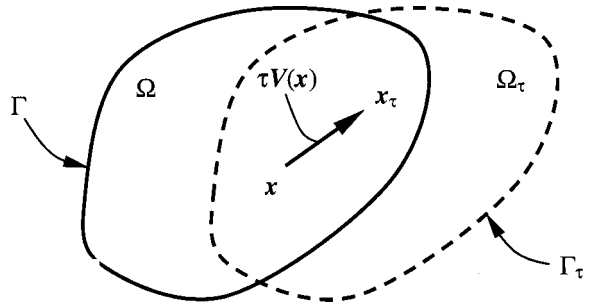

Fig. 1 Variation of domain

In the neighborhood of an initial time $\tau=0$, assuming a regularity hypothesis and ignoring high-order terms, $\mathbf{T}$ can be approximated by

$$\mathbf{T}(\mathbf{x},\tau)=\mathbf{T}(\mathbf{x},0)+\tau\frac{\partial\mathbf{T}(\mathbf{x},0)}{\partial\tau}+O(\tau^2)\cong\mathbf{x}+\tau\mathbf{V}(\mathbf{x},0) \tag{4}$$

where $\mathbf{x}=\mathbf{T}(\mathbf{x},0)$ and $\mathbf{V}(\mathbf{x})=\mathbf{V}(\mathbf{x},0)$

Shape Sensitivity Analysis. The variational governing equation for a structural component with domain Ω can be formulated as [11]

$$a_\Omega(z,\overline{z})=\ell_\Omega(\overline{z}),\quad \text{for all } \overline{z}\in Z \tag{5}$$

where $\mathbf{z}$ and $\overline{\mathbf{z}}$ are the actual displacement and virtual displacement fields of the structure, respectively, $\mathbf{Z}$ is the space of kinematically admissible virtual displacements, and $a_\Omega(\mathbf{z},\overline{\mathbf{z}})$ and $\ell_\Omega(\overline{\mathbf{z}})$ are energy bilinear and load linear forms, respectively. The subscript Ω in Eq. (5) is used to indicate the dependency of the governing equation on the shape of the structural domain.

The pointwise material derivative at $\mathbf{x}\in\Omega$ is defined as [11]

$$\dot{\mathbf{z}}=\lim_{\tau\to0}\left[\frac{\mathbf{z}_\tau(\mathbf{x}+\tau\mathbf{V}(\mathbf{x}))-\mathbf{z}(\mathbf{x})}{\tau}\right] \tag{6}$$

If $\mathbf{z}_\tau$ has a regular extension to a neighborhood of Ω_τ, then

$$\dot{\mathbf{z}}(\mathbf{x})=\mathbf{z}'(\mathbf{x})+\nabla\mathbf{z}^T\mathbf{V}(\mathbf{x}) \tag{7}$$

where

$$\mathbf{z}'=\lim_{\tau\to0}\left[\frac{\mathbf{z}_\tau(\mathbf{x})-\mathbf{z}(\mathbf{x})}{\tau}\right] \tag{8}$$

is the partial derivative of $\mathbf{z}$ and $\nabla=\{\partial/\partial x_1,\partial/\partial x_2,\partial/\partial x_3\}^T$ is the vector of gradient operators. One attractive feature of the partial derivative is that, given the smoothness assumption, it commutes with the derivatives with respect to x_i, $i=1$, 2, and 3, since they are derivatives with respect to independent variables, i.e.,

$$\left(\frac{\partial\mathbf{z}}{\partial x_i}\right)'=\frac{\partial}{\partial x_i}(\mathbf{z}'),\quad i=1,\ 2,\ \text{and}\ 3 \tag{9}$$

Let ψ_1 be a domain functional, defined as an integral over Ω_τ, i.e.,

$$\psi_1=\int_{\Omega_\tau}f_\tau(\mathbf{x}_\tau)d\Omega_\tau \tag{10}$$

where f_τ is a regular function defined on Ω_τ. If Ω is C^k regular, then the material derivative of ψ_1 at Ω is [11]

$$\dot{\psi}_1=\int_\Omega[f'(\mathbf{x})+\text{div}(f(\mathbf{x})\mathbf{V}(\mathbf{x}))]d\Omega \tag{11}$$

For a functional form of

$$\psi_2=\int_{\Omega_\tau}g(\mathbf{z}_\tau,\nabla\mathbf{z}_\tau)d\Omega_\tau \tag{12}$$

the material derivative of ψ_2 at Ω using Eqs. (9) and (11) is

$$\dot{\psi}_2=\int_\Omega[g_{,z_i}\dot{z}_i-g_{,z_i}(z_{i,j}V_j)+g_{,z_{i,j}}\dot{z}_{i,j}-g_{,z_{i,j}}(z_{i,j}V_j)_{,j}+\text{div}(g\mathbf{V})]d\Omega \tag{13}$$

for which a comma is used to denote partial differentiation, e.g., $z_{i,j}=\partial z_i/\partial x_j$, $\dot{z}_{i,j}=\partial\dot{z}_i/\partial x_j$, $g_{,z_i}=\partial g/\partial z_i$, $g_{,z_{i,j}}=\partial g/\partial z_{i,j}$ and V_j is the jth component of $\mathbf{V}$. In Eq. (13), the material derivative $\dot{\mathbf{z}}$ is the solution of the sensitivity equation obtained by taking the material derivative of Eq. (5).

If no body force is involved, the variational equation (Eq. (5)) can be written as

$$a_\Omega(\mathbf{z},\overline{\mathbf{z}})\equiv\int_\Omega\sigma_{ij}(\mathbf{z})\varepsilon_{ij}(\overline{\mathbf{z}})d\Omega=\ell_\Omega(\overline{\mathbf{z}})\equiv\int_\Gamma T_i\overline{z}_i d\Gamma \tag{14}$$

where $\sigma_{ij}(z)$ and $\varepsilon_{ij}(\overline{z})$ are the stress and strain tensors of the displacement z and virtual displacement $\overline{z}$, respectively, T_i is the ith component of the surface traction, and $\overline{z}_i$ is the ith component of $\overline{z}$. Taking the material derivative of both sides of Eq. (14) and using Eqs. (7)–(9)

$$a_\Omega(\dot{\mathbf{z}},\overline{\mathbf{z}})=\ell'_{\mathbf{V}}(\overline{\mathbf{z}})-a'_{\mathbf{V}}(\mathbf{z},\overline{\mathbf{z}}),\quad \forall\overline{\mathbf{z}}\in\mathbf{Z} \tag{15}$$

where the subscript V indicates the dependency of the terms on the velocity field. The terms $\ell'_V(\overline{z})$ and $a'_V(z,\overline{z})$ can be further derived as [11]

$$\ell'_{\mathbf{V}}(\overline{\mathbf{z}})=\int_\Gamma\{-T_i(z_{i,j}V_j)+[(T_i\overline{z}_i)_{,j}n_j+\kappa_\Gamma(T_i\overline{z}_i)](V_in_i)\}d\Gamma \tag{16}$$

and

$$a'_{\mathbf{V}}(\mathbf{z},\overline{\mathbf{z}})=-\int_\Omega[\sigma_{ij}(\mathbf{z})(\overline{z}_{i,k}V_{k,j})+\sigma_{ij}(\overline{\mathbf{z}})(z_{i,k}V_{k,j})-\sigma_{ij}(\mathbf{z})\varepsilon_{ij}(\overline{\mathbf{z}})\text{div}\,\mathbf{V}]d\Omega \tag{17}$$

where n_i is the ith component of unit normal vector n, κ_Γ is the curvature of the boundary, $\overline{z}_{i,j}=\partial\overline{z}_i/\partial x_j$, and $V_{i,j}=\partial V_i/\partial x_j$.

To evaluate the sensitivity expression in Eq. (13), a numerical method is needed to solve $\dot{\mathbf{z}}$ in Eq. (15). In this study, the standard FEM was used. If the solution $\mathbf{z}$ of Eq. (14) is obtained using an FEM code, the same code can be used to solve Eq. (15) for $\dot{\mathbf{z}}$. This solution of $\dot{\mathbf{z}}$ can be obtained efficiently since it requires only the evaluation of the same set of FEM matrix equations with a different fictitious load, which is the right-hand side of Eq. (15). In other words, $\dot{\mathbf{z}}$ can be solved using the same stiffness matrix from the unperturbed FEM mesh. There is no need to calculate the derivative of the stiffness matrix, as required in virtual crack extension methods. In this study, the ABAQUS [13] finite element code (Version 5.8) was used in all numerical calculations presented in a forthcoming section.

The *J*-integral

Consider a body with a crack of length a, subject to mode-I loading. Using an arbitrary counterclockwise path Γ around the crack tip, as shown in Fig. 2(*a*), a formal definition of J under mode-I condition is [14]

$$J\overset{\text{def}}{=}\int_\Gamma(Wn_1-T_iz_{i,1})ds \tag{18}$$

where $W=\int\sigma_{ij}d\varepsilon_{ij}$ is the strain energy density, $T_i=\sigma_{ij}n_j$, ds is the differential length along contour Γ, and $z_{i,1}=\partial z_i/\partial x_1$. The summation convention is adopted here for repeated indices.

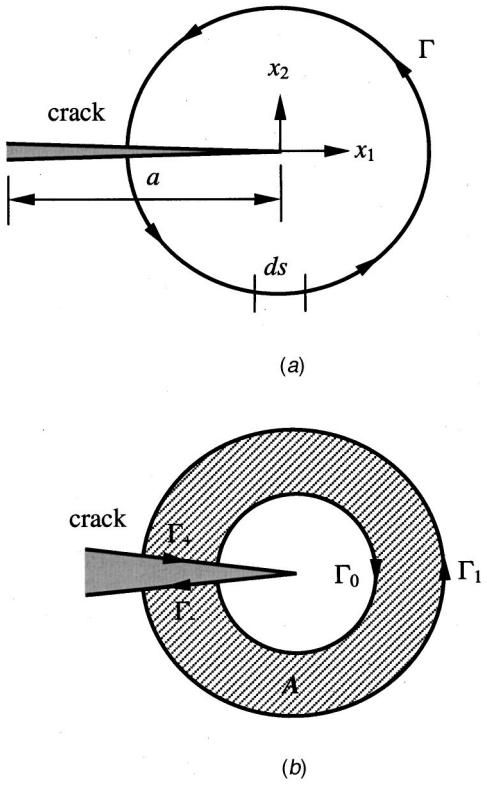

Fig. 2 *J*-integral fracture parameter—(*a*) arbitrary contour around a crack tip; (*b*) inner and outer contours enclosing *A*

Using the divergence theorem, the contour integral defined in Eq. (18) can be expanded into an area integral in two dimensions, and volume integral in three dimensions, over a finite domain surrounding the crack tip or crack front. For two-dimensional problems involving linear- or nonlinear-elastic material under quasi-static conditions, in the absence of body forces, thermal strains, and crack-face tractions, Eq. (18) reduces to [15]

$$J=\int_A\left[\sigma_{ij}\frac{\partial z_j}{\partial x_1}-W\delta_{1i}\right]\frac{\partial q}{\partial x_i}dA, \tag{19}$$

where δ_{1i} is the Kronecker delta, q is an arbitrary but smooth weighting function equal to *unity* on Γ_0 and *zero* on Γ_1, and A is the annular area enclosed by the inner contour Γ_0 and outer contour Γ_1, as shown in Fig. 2(*b*). In this study, the inner contour Γ_0 coincides with the crack tip. Hence, A becomes the area inside the outer contour Γ_1. On further expansion

$$J=\int_A\left[\left(\sigma_{11}\frac{\partial z_1}{\partial x_1}+\sigma_{12}\frac{\partial z_2}{\partial x_1}\right)\frac{\partial q}{\partial x_1}+\left(\sigma_{21}\frac{\partial z_1}{\partial x_1}+\sigma_{22}\frac{\partial z_2}{\partial x_1}\right)\frac{\partial q}{\partial x_2}-W\frac{\partial q}{\partial x_1}\right]dA \tag{20}$$

where

$$W=\int_0^{\varepsilon_{ij}}\sigma_{ij}d\varepsilon_{ij}$$
$$=\begin{cases}\left(\frac{E}{1-\nu^2}\right)\left(\frac{\varepsilon_{11}^2}{2}+\nu\varepsilon_{11}\varepsilon_{22}\right)+\left(\frac{E}{1+\nu}\right)\varepsilon_{12}^2 \\ \quad+\left(\frac{E}{1-\nu^2}\right)\left(\frac{\varepsilon_{22}^2}{2}+\nu\varepsilon_{11}\varepsilon_{22}\right), \qquad \text{for plane stress} \\ \left(\frac{E}{(1-2\nu)(1+\nu)}\right)\left(\frac{(1-\nu)\varepsilon_{11}^2}{2}+2\nu\varepsilon_{11}\varepsilon_{22}+\frac{(1-\nu)\varepsilon_{22}^2}{2}\right) \\ \quad+\left(\frac{E}{1+\nu}\right)\varepsilon_{12}^2, \qquad \text{for plane strain}\end{cases} \tag{21}$$

E is the Young's modulus, ν is the Poisson's ratio for the material of the body, and ε_{ij} is the strain field given by

$$\varepsilon_{ij}=\frac{1}{2}\left(\frac{\partial z_i}{\partial x_j}+\frac{\partial z_j}{\partial x_i}\right), \quad i,j=1,2 \tag{22}$$

Sensitivity of the *J*-integral

For two-dimensional plane stress or plane strain problems, once the stress-strain relationship is applied, Eq. (20) can be expressed as

$$J=\int_A h dA \tag{23}$$

where

$$h=h_1+h_2+h_3+h_4-h_5-h_6 \tag{24}$$

The explicit expressions of h_i, $i=1,\ldots,6$ are given in Appendix A for both plane stress and plane strain conditions. In relation to Eq. (11), the material derivative of the *J*-integral is

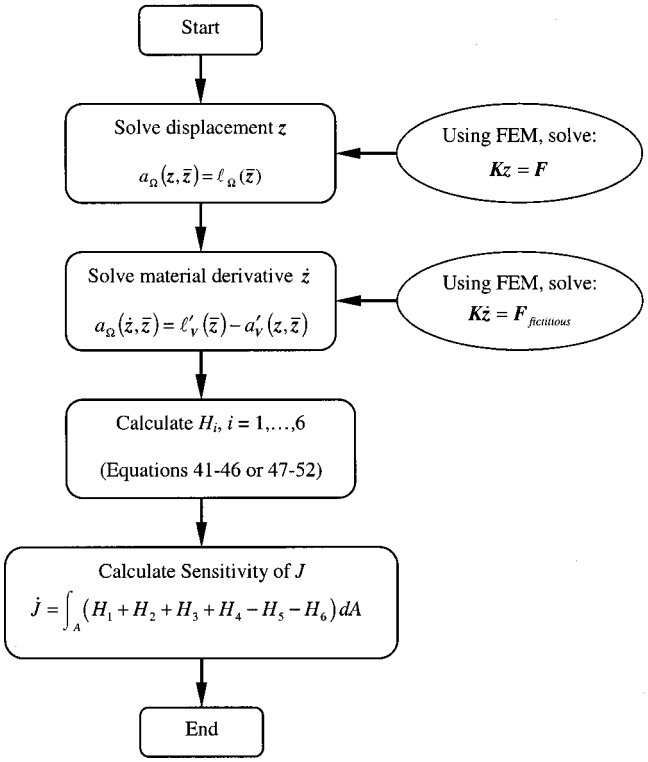

Fig. 3 A flowchart for continuum sensitivity analysis of crack size

$$\dot{J} = \int_A [h' + \mathrm{div}(h\mathbf{V})]dA \tag{25}$$

where

$$h' = h_1' + h_2' + h_3' + h_4' - h_5' - h_6' \tag{26}$$

and $\mathbf{V} = \{V_1, V_2\}^T$. Assuming the crack length a to be the variable of interest, a change in crack length in the x_1 direction (mode-I) only, i.e., $\mathbf{V} = \{V_1, 0\}^T$, results in the expression of Eq. (25) as

$$\dot{J} = \int_A (H_1 + H_2 + H_3 + H_4 - H_5 - H_6)dA \tag{27}$$

where

$$H_i = h_i' + \frac{\partial(h_i V_1)}{\partial x_1}, \quad i = 1, \ldots, 6 \tag{28}$$

Equations (41)–(46) and (47)–(52) in Appendix B provide explicit expressions of H_i, $i = 1,6$, for plane stress and plane strain conditions, respectively. These expressions of H_i, $i = 1,6$, when inserted in Eq. (27), yield the first-order sensitivity of J with respect to crack size. Note, when the velocity field is unity at the crack tip, $\dot{J}$ is equal to $\partial J/\partial a$.

Numerical integration is required in calculating both J (Eq. (19)) and $\partial J/\partial a$ (Eq. (27)). Since Eq. (19) is already coded in ABAQUS, J can be obtained readily. However, Eq. (27) is new and is currently not available in ABAQUS. Hence, new subroutines were developed to calculate $\partial J/\partial a$. They involve calculating the H-functions (Eqs. (41)–(52)) using the ABAQUS-generated displacement/strain fields and then performing numerical integration in Eq. (27). Note, the integral in Eq. (27) is independent of the domain size A and was calculated numerically using the standard Gaussian quadrature. A 2×2 or higher integration rule is recommended to calculate $\dot{J}$ or $\partial J/\partial a$. A flow diagram for calculating the sensitivity of J is shown in Fig. 3.

Numerical Examples

Example 1: M(T) Specimen. Consider a middle-tension [M(T)] specimen with width $2W = 20$ units, length $2L = 20$ units and crack length $2a$, subjected to a far-field remote tensile stress, $\sigma^\infty = 1$ unit. Two crack sizes with normalized crack lengths $a/W = 0.025$ and 0.05 were considered. The elastic modulus E and Poisson's ratio ν were 26 units and 0.3, respectively.

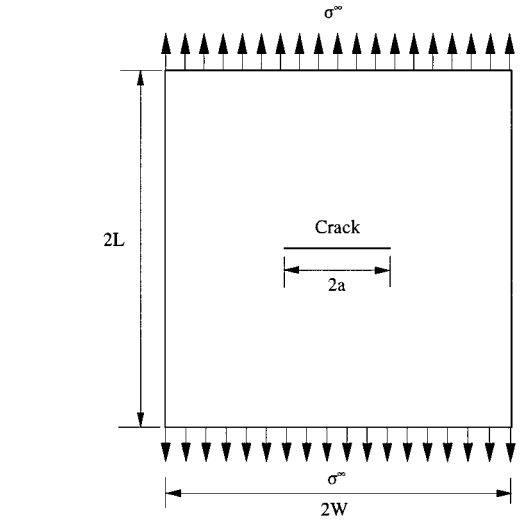

(*a*)

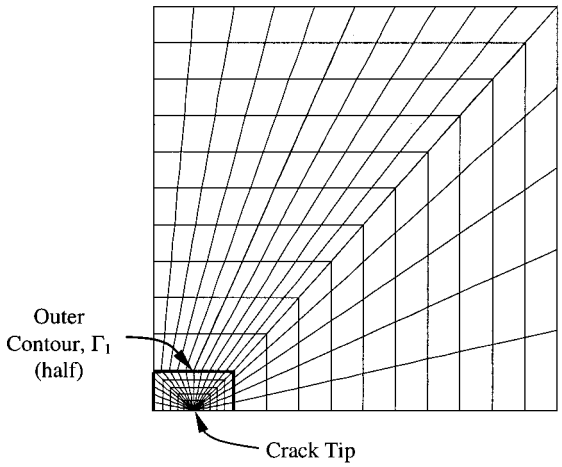

(*b*)

Fig. 4 M(T) specimen under mode-I loading—(*a*) geometry and loads; (*b*) finite element mesh (1/4 model)

Table 1 Sensitivity of *J* for M(T) specimen by the proposed and analytical methods

		Sensitivity of *J*-integral ($\partial J/\partial a$)		
a/W	*J*-integral	Proposed Method	Analytical Method	Difference[(a)] (percent)
		(*a*) plane stress		
0.025	3.04×10^{-5}	1.22×10^{-4}	1.21×10^{-4}	-0.83
0.05	6.01×10^{-5}	1.19×10^{-4}	1.21×10^{-4}	1.65
		(*b*) plane strain		
0.025	2.77×10^{-5}	1.12×10^{-4}	1.10×10^{-4}	-1.82
0.05	5.48×10^{-5}	1.13×10^{-4}	1.10×10^{-4}	-2.72

(a) Difference = ($\partial J/\partial a$ by analytical method - $\partial J/\partial a$ by proposed method)$\times100/\partial J/\partial a$ by analytical method

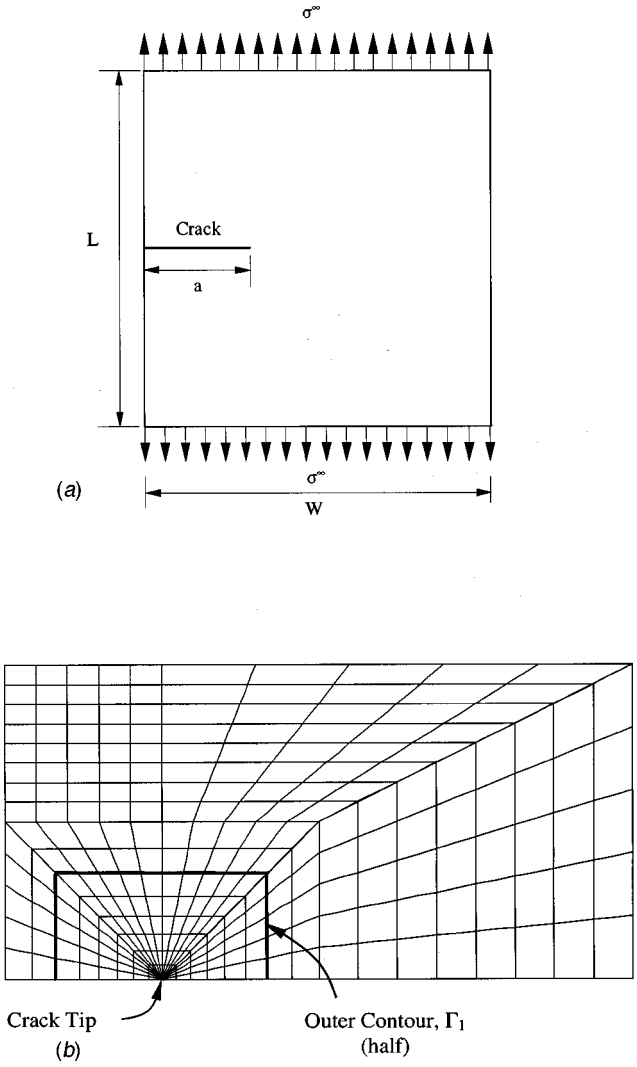

Fig. 5 SE(T) specimen under mode-I loading—(*a*) geometry and loads; (*b*) finite element mesh (1/2 model)

Figure 4(*a*) shows the geometry and loads of the M(T) specimen. A finite element mesh for 1/4-model was used due to the double-symmetry of this M(T) problem, as shown in Fig. 4(*b*). Both plane stress and plane strain conditions were studied. Second-order elements from the ABAQUS (Version 5.8) [13] element library were employed. For plane stress, the element type was CPS8R—the reduced integration, eight-noded quadrilateral element. The element-type CPE8R was used for plane strain. The model consisted of 270 elements and 843 nodes. Focused elements with collapsed nodes were employed in the vicinity of crack tip. The domain (contour) of integration is depicted in Fig. 4(*b*). A 2×2 Gaussian integration was used.

Table 1 presents the numerical results for J and $\partial J/\partial a$ for the M(T) problem. Both plane stress and plane strain conditions were analyzed. For each stress state, two sets of results are shown for $\partial J/\partial a$. The first set presents $\partial J/\partial a$ computed using the method described herein; the second set was calculated using the analytical solution for an infinite plate [15]. The results in Table 1 demonstrate that the continuum shape sensitivity analysis provides very accurate results for $\partial J/\partial a$ in comparison with the corresponding results from the analytical solution. Unlike the virtual crack extension technique, no mesh perturbation is required in the proposed method. The difference between the results of the proposed method and the analytical solution is less than 3%. A relatively larger difference in results for $a/W=0.05$ is due to the use of analytical solution, which is strictly valid when $a/W\rightarrow 0$.

Example 2: SE(T) Specimen. Consider a single-edged-tension [SE(T)] specimen with width $W=10$ units, length $L=10$ units, and crack length a, subjected to a far-field remote tensile stress $\sigma^{\infty}=1$ unit. Two crack sizes with normalized crack lengths $a/W=0.25$ and 0.5 were considered. The elastic modulus E and Poisson's ratio ν were 30 units and $\nu=0.25$, respectively.

The geometry and loads of the SE(T) specimen are shown in Fig. 5(*a*). Due to single-symmetry of the SE(T) problem, a finite element mesh for 1/2-model was used, as shown in Fig. 5(*b*). The model consisted of 280 elements and 873 nodes. As before, both plane stress and plane strain conditions were studied.

Table 2 presents the numerical results for J and $\partial J/\partial a$ for the SE(T) problem. Two sets of results are shown for $\partial J/\partial a$, the first computed using the proposed method and second calculated using the finite-difference method, since no analytical solution was available for this problem. A 1% perturbation of crack length was used in the finite-difference calculations. As in Example 1, the results in Table 2 also demonstrate that continuum shape sensitivity analysis provides accurate estimates of $\partial J/\partial a$ as compared with corresponding results from the finite-difference method. Unlike the virtual crack extension technique, no mesh perturbation is required using the proposed method. The difference between the results of the proposed method and the finite-difference method is less than 2%.

Table 2 Sensitivity of *J* for SE(T) specimen by the proposed and finite-difference methods

		Sensitivity of *J*-integral ($\partial J/\partial a$)		
a/W	*J*-integral	Proposed Method	Finite Difference	Difference[(a)] (percent)
		(*a*) plane stress		
0.25	5.80×10^{-7}	4.63×10^{-7}	4.59×10^{-7}	- 0.87
0.5	4.70×10^{-6}	3.48×10^{-7}	3.54×10^{-7}	1.69
		(*b*) plane strain		
0.25	5.44×10^{-7}	4.28×10^{-7}	4.30×10^{-7}	0.65
0.5	4.39×10^{-6}	3.52×10^{-7}	3.49×10^{-7}	-0.86

(a) Difference = ($\partial J/\partial a$ by finite difference method - $\partial J/\partial a$ by proposed method)×100/$\partial J/\partial a$ by finite difference method

Conclusions

A new method was developed for shape sensitivity analysis of a crack in a homogeneous, isotropic, and linear-elastic body subject to mode-I loading. The method involves the material derivative concept of continuum mechanics, domain integral representation of the *J*-integral, and direct differentiation. Unlike virtual crack extension techniques, no mesh perturbation is required in the proposed method. Since the governing variational equation is differentiated prior to the process of discretization, the resulting sensitivity equations are independent of any approximate numerical techniques, such as the finite element method, boundary element method, or others. Existing methods based on the expression of *J* as a rate of potential energy require second-order sensitivity of potential energy to yield the first-order sensitivity of *J*. Since the proposed method requires only first-order sensitivity of displacement field, it is much simpler and more efficient than existing methods. Numerical results demonstrate that the maximum difference in calculating the sensitivity of *J* using the developed method is less than 3%, compared with the analytical solution or finite-difference results.

Acknowledgments

This research was supported by the Faculty Early Career Development Award (second author) of the U.S. National Science Foundation (Grant No. CMS-9733058). The NSF program directors were Drs. Sunil Saigal and Ken Chong.

Appendix A

The *h* Functions. For plane stress

$$h_1=\frac{E}{1-\nu^2}\frac{\varepsilon_{11}^2}{2}\frac{\partial q}{\partial x_1} \tag{29}$$

$$h_2=\frac{E}{1+\nu}\varepsilon_{12}\frac{\partial z_2}{\partial x_1}\frac{\partial q}{\partial x_1} \tag{30}$$

$$h_3=\frac{E}{1+\nu}\varepsilon_{12}\varepsilon_{11}\frac{\partial q}{\partial x_2} \tag{31}$$

$$h_4=\frac{E}{1-\nu^2}(\varepsilon_{22}+\nu\varepsilon_{11})\frac{\partial z_2}{\partial x_1}\frac{\partial q}{\partial x_2} \tag{32}$$

$$h_5=\frac{E}{1+\nu}\varepsilon_{12}^2\frac{\partial q}{\partial x_1} \tag{33}$$

and

$$h_6=\frac{E}{1-\nu^2}\left(\frac{\varepsilon_{22}^2}{2}+\nu\varepsilon_{11}\varepsilon_{22}\right)\frac{\partial q}{\partial x_1} \tag{34}$$

For plane strain

$$h_1=\frac{E(1-\nu)}{(1+\nu)(1-2\nu)}\frac{\varepsilon_{11}^2}{2}\frac{\partial q}{\partial x_1} \tag{35}$$

$$h_2=\frac{E}{1+\nu}\varepsilon_{12}\frac{\partial z_2}{\partial x_1}\frac{\partial q}{\partial x_1} \tag{36}$$

$$h_3=\frac{E}{1+\nu}\varepsilon_{12}\varepsilon_{11}\frac{\partial q}{\partial x_2} \tag{37}$$

$$h_4=\frac{E}{(1+\nu)(1-2\nu)}[(1-\nu)\varepsilon_{22}+\nu\varepsilon_{11}]\frac{\partial z_2}{\partial x_1}\frac{\partial q}{\partial x_2} \tag{38}$$

$$h_5=\frac{E}{1+\nu}\varepsilon_{12}^2\frac{\partial q}{\partial x_1} \tag{39}$$

and

$$h_6=\frac{E}{(1+\nu)(1-2\nu)}\left[\frac{\varepsilon_{22}^2}{2}(1-\nu)+\nu\varepsilon_{11}\varepsilon_{22}\right]\frac{\partial q}{\partial x_1} \tag{40}$$

Appendix B

The *H* Functions. For plane stress

$$H_1=\frac{E}{1-\nu^2}\frac{\partial q}{\partial x_1}\left[\varepsilon_{11}\frac{\partial \dot z_1}{\partial x_1}-\varepsilon_{11}^2\frac{\partial V_1}{\partial x_1}\right] \tag{41}$$

$$H_2=\frac{E}{1+\nu}\frac{\partial q}{\partial x_1}\left[\frac{\partial z_2}{\partial x_1}\left(\frac{\partial \dot z_2}{\partial x_1}+\frac{1}{2}\frac{\partial \dot z_1}{\partial x_2}-\frac{1}{2}\varepsilon_{11}\frac{\partial V_1}{\partial x_2}-\frac{\partial z_2}{\partial x_1}\frac{\partial V_1}{\partial x_1}\right)+\frac{1}{2}\frac{\partial z_1}{\partial x_2}\left(\frac{\partial \dot z_2}{\partial x_1}-\frac{\partial z_2}{\partial x_1}\frac{\partial V_1}{\partial x_1}\right)\right] \tag{42}$$

$$H_3=\frac{1}{2}\frac{E}{1+\nu}\frac{\partial q}{\partial x_2}\left[\varepsilon_{11}\left(\frac{\partial \dot z_2}{\partial x_1}+\frac{\partial \dot z_1}{\partial x_2}\right)+2\varepsilon_{12}\frac{\partial \dot z_1}{\partial x_1}-\varepsilon_{11}^2\frac{\partial V_1}{\partial x_2}-\varepsilon_{11}\frac{\partial z_2}{\partial x_1}\frac{\partial V_1}{\partial x_1}\right]-\varepsilon_{11}\varepsilon_{12}\frac{E}{1+\nu}\frac{\partial q}{\partial x_1}\frac{\partial V_1}{\partial x_2} \tag{43}$$

$$H_4=\frac{E}{1-\nu^2}\frac{\partial q}{\partial x_2}\frac{\partial z_2}{\partial x_1}\left(\frac{\partial \dot z_2}{\partial x_2}+\nu\frac{\partial \dot z_1}{\partial x_1}\right)-\frac{E}{1-\nu^2}\frac{\partial q}{\partial x_2}\times\left[\left(\frac{\partial z_2}{\partial x_1}\right)^2\frac{\partial V_1}{\partial x_2}+\nu\varepsilon_{11}\frac{\partial z_2}{\partial x_1}\frac{\partial V_1}{\partial x_1}\right]+\frac{E}{1-\nu^2}(\varepsilon_{22}+\nu\varepsilon_{11})\times\left[\frac{\partial q}{\partial x_2}\frac{\partial \dot z_2}{\partial x_1}-\frac{\partial q}{\partial x_1}\frac{\partial z_2}{\partial x_1}\frac{\partial V_1}{\partial x_2}\right] \tag{44}$$

$$H_5=\frac{E}{1+\nu}\frac{\partial q}{\partial x_1}\varepsilon_{12}\left[\frac{\partial \dot z_1}{\partial x_2}+\frac{\partial \dot z_2}{\partial x_1}-\frac{\partial z_2}{\partial x_1}\frac{\partial V_1}{\partial x_1}-\varepsilon_{11}\frac{\partial V_1}{\partial x_2}\right] \tag{45}$$

and

$$H_6=\frac{E}{1-\nu^2}\frac{\partial q}{\partial x_1}\left[(\varepsilon_{22}+\nu\varepsilon_{11})\left(\frac{\partial \dot z_2}{\partial x_2}-\frac{\partial z_2}{\partial x_1}\frac{\partial V_1}{\partial x_2}\right)+\nu\varepsilon_{22}\left(\frac{\partial \dot z_1}{\partial x_1}-\varepsilon_{11}\frac{\partial V_1}{\partial x_1}\right)\right] \tag{46}$$

For plane strain

$$H_1=\frac{E(1-\nu)}{(1-2\nu)(1+\nu)}\frac{\partial q}{\partial x_1}\left[\varepsilon_{11}\frac{\partial \dot z_1}{\partial x_1}-\varepsilon_{11}^2\frac{\partial V_1}{\partial x_1}\right] \tag{47}$$

$$H_2=\frac{E}{1+\nu}\frac{\partial q}{\partial x_1}\left[\frac{\partial z_2}{\partial x_1}\left(\frac{\partial \dot z_2}{\partial x_1}+\frac{1}{2}\frac{\partial \dot z_1}{\partial x_2}-\frac{1}{2}\varepsilon_{11}\frac{\partial V_1}{\partial x_2}-\frac{\partial z_2}{\partial x_1}\frac{\partial V_1}{\partial x_1}\right)+\frac{1}{2}\frac{\partial z_1}{\partial x_2}\left(\frac{\partial \dot z_2}{\partial x_1}-\frac{\partial z_2}{\partial x_1}\frac{\partial V_1}{\partial x_1}\right)\right] \tag{48}$$

$$H_3=\frac{1}{2}\frac{E}{1+\nu}\frac{\partial q}{\partial x_2}\left[\varepsilon_{11}\left(\frac{\partial \dot z_2}{\partial x_1}+\frac{\partial \dot z_1}{\partial x_2}\right)+2\varepsilon_{12}\frac{\partial \dot z_1}{\partial x_1}-\varepsilon_{11}^2\frac{\partial V_1}{\partial x_2}-\varepsilon_{11}\frac{\partial z_2}{\partial x_1}\frac{\partial V_1}{\partial x_1}\right]-\varepsilon_{11}\varepsilon_{12}\frac{E}{1+\nu}\frac{\partial q}{\partial x_1}\frac{\partial V_1}{\partial x_2} \tag{49}$$

$$H_4=\frac{E}{(1-2\nu)(1+\nu)}\frac{\partial q}{\partial x_2}\frac{\partial z_2}{\partial x_1}\left[\nu\left(\frac{\partial \dot z_1}{\partial x_1}-\varepsilon_{11}\frac{\partial V_1}{\partial x_1}\right)+(1-\nu)\times\left(\frac{\partial \dot z_2}{\partial x_2}-\frac{\partial z_2}{\partial x_1}\frac{\partial V_1}{\partial x_2}\right)\right]+\frac{E}{(1-2\nu)(1+\nu)}[(1-\nu)\varepsilon_{22}+\nu\varepsilon_{11}]\times\left[\frac{\partial q}{\partial x_2}\frac{\partial \dot z_2}{\partial x_1}-\frac{\partial z_2}{\partial x_1}\frac{\partial q}{\partial x_1}\frac{\partial V_1}{\partial x_2}\right] \tag{50}$$

$$H_5=\frac{E}{1+\nu}\frac{\partial q}{\partial x_1}\varepsilon_{12}\left[\frac{\partial \dot z_1}{\partial x_2}+\frac{\partial \dot z_2}{\partial x_1}-\varepsilon_{11}\frac{\partial V_1}{\partial x_2}-\frac{\partial z_2}{\partial x_1}\frac{\partial V_1}{\partial x_1}\right] \tag{51}$$

and

$$H_6=\frac{E}{(1-2\nu)(1+\nu)}\frac{\partial q}{\partial x_1}\left[((1-\nu)\varepsilon_{22}+\nu\varepsilon_{11})\left(\frac{\partial \dot{z}_2}{\partial x_2}-\frac{\partial z_2}{\partial x_1}\frac{\partial V_1}{\partial x_2}\right)+\nu\varepsilon_{22}\left(\frac{\partial \dot{z}_1}{\partial x_1}-\varepsilon_{11}\frac{\partial V_1}{\partial x_1}\right)\right] \quad (52)$$

References

[1] Madsen, H. O., Krenk, S., and Lind, N. C., 1986, *Methods of Structural Safety*, Prentice-Hall, Inc., Englewood Cliffs, NJ.

[2] Provan, J. W., 1987, *Probabilistic Fracture Mechanics and Reliability*, Martinus Nijhoff Publishers, Dordrecht, The Netherlands.

[3] Rahman, S., 1995, ''A Stochastic Model for Elastic-Plastic Fracture Analysis of Circumferential Through-Wall-Cracked Pipes Subject to Bending,'' Eng. Fract. Mech., **52**(2), pp. 265–288.

[4] Rahman, S., 2001, ''Probabilistic Fracture Mechanics by *J*-estimation and Finite Element Methods,'' Eng. Fract. Mech., **68**, pp. 107–125.

[5] Lin, S. C., and Abel, J., 1988, ''Variational Approach for a New Direct-Integration Form of the Virtual Crack Extension Method,'' Int. J. Fract., **38**, pp. 217–235.

[6] deLorenzi, H. G., 1985, ''Energy Release Rate Calculations by the Finite Element Method,'' Eng. Fract. Mech., **21**, pp. 129–143.

[7] Haber, R. B., and Koh, H. M., 1985, ''Explicit Expressions for Energy Release Rates using Virtual Crack Extensions,'' Int. J. Numer. Methods Eng., **21**, pp. 301–315.

[8] Barbero, E. J., and Reddy, J. N., 1990, ''The Jacobian Derivative Method for Three-Dimensional Fracture Mechanics,'' Commun. Appl. Numer. Methods, **6**, pp. 507–518.

[9] Hwang, C. G., Wawrzynek, P. A., Tayebi, A. K., and Ingraffea, A. R., 1998, ''On the Virtual Crack Extension Method for Calculation of the Rates of Energy Release Rate,'' Eng. Fract. Mech., **59**, pp. 521–542.

[10] Feijóo, R. A., Padra, C., Saliba, R., Taroco, E., and Vénere, M. J., 2000, ''Shape Sensitivity Analysis for Energy Release Rate Evaluations and Its Application to the Study of Three-Dimensional Cracked Bodies,'' Comput. Methods Appl. Mech. Eng., **188**, pp. 649–664.

[11] Haug, E. J., Choi, K. K., and Komkov, V., 1986, *Design Sensitivity Analysis of Structural Systems*, Academic Press, New York, NY.

[12] Taroco, E., 2000, ''Shape Sensitivity Analysis in Linear Elastic Cracked Structures,'' Comput. Methods Appl. Mech. Eng., **188**, pp. 697–712.

[13] ABAQUS, 1999, *User's Guide and Theoretical Manual*, Version 5.8, Hibbitt, Karlsson, and Sorenson, Inc., Pawtucket, RI.

[14] Rice, J. R., 1968, ''A Path Independent Integral and the Approximate Analysis of Strain Concentration by Notches and Cracks,'' ASME J. Appl. Mech., **35**, pp. 379–386.

[15] Anderson, T. L., 1995, *Fracture Mechanics: Fundamentals and Applications*, Second Edition, CRC Press, Inc., Boca Raton, FL.